



This is the accepted manuscript made available via CHORUS. The article has been published as:

First-principles electronic structure in second-moment calculation of mode frequencies: Failure of quasiharmonic approximation in silicon

Doyl Dickel and Murray S. Daw

Phys. Rev. B **100**, 214314 — Published 27 December 2019

DOI: 10.1103/PhysRevB.100.214314

First-principles electronic structure in second-moment calculation of mode frequencies: failure of quasiharmonic approximation in silicon

Doyl Dickel¹ and Murray S. Daw²

¹Center for Advanced Vehicular Systems,

Mississippi State University Starkville, MS 39759

²Department of Physics and Astronomy,

Clemson University, SC, USA 29634-0978

Abstract

For the first time using first-principles electronic structure calculations (LDA), we present secondmoment calculations of the temperature-dependence of the vibrational normal mode frequencies in Si up to 1500K. The method is based on simple ensemble averages of displacements and forces and
is easy to implement. These efficient calculations incorporate all interactions nonperturbatively,
implicitly including all high order force constants, in contrast to typical perturbative approaches.

Also new to this work, we propose and apply to our classical calculations an estimated quantum
correction that could be used for classical approaches other than the moments method. We compare our results to available experiments, including recent inelastic neutron scattering data and
conclude that the second-moment gives the frequency shift to within a factor of 2 in contrast to
quasi-harmonic approaches which fail by an order of magnitude to predict the anharmonic shift.

Noting the relative simplicity and speed of the calculations, we conclude that the second-moment
approximation reasonably accounts for anharmonicity in a system that has been very closely studied experimentally and may reliably be applied in an exploratory way to more complex systems.

We suggest that further improvement on the results could be obtained by incorporating the fourth
moment, which can be implemented with little additional cost.

PACS numbers: 34.20.Cf, 63.20.dk, 63.20.D-, 63.20.Ry, 63.20.kg, 71.36.+c

I. INTRODUCTION

The frequencies of the vibrational modes of Si downshift with increasing temperature at a rate that is much larger than expected from the quasiharmonic approximation – that is, by thermal expansion alone. The experimental shifts have been measured by Raman experiments [1–3] and by neutron scattering [4–6]. In particular, Kim *et al.* conclude that the shifts are dominanted by anharmonic effects beyond the quasiharmonic approximation.

In this paper we use the well-explored case of the temperature-dependence of the vibrational mode frequencies in Si as a proving ground for an approximate, relatively simple method of calculating anharmonic effects which we refer to as a "moments approximation".

We have employed the second-moment approximation in previous work to study the temperature-dependent shift of modes using the Tersoff potential. For example, we studied the frequency shifts for carbon nanotubes [7] and fullerenes [8]; the predicted temperature-dependent shift of the frequencies for modes of carbon nanotubes and fullerenes are within a factor of 2 in agreement with experiment, mostly Raman spectroscopy. Using the same method, we performed a careful evaluation of subtleties of anharmonicity of graphene [9]. In this case, the flexural (out-of-plane) modes couple anharmonically to in-plane modes, causing a temperature-dependent renormalization of the dispersion of the flexural modes, which is an essential contribution to the stabilization of graphene sheets. These prior successes give us confidence that the second-moment approximation should give reasonable agreement with experiment in the present application.

By contrast, this paper reports the application of the moments method using first-principles LDA to determine the energies and forces. We will discuss in this paper several considerations that crop up as a result of using a first-principles electronic structure calculation. In addition, this type of calculation is more computationally intensive than those based on interatomic potentials, and so it is helpful to have the direct comparison available which we make here. In general, the first-principles energies and forces are more reliable, especially at higher temperatures.

We do two separate sets of second-moment calculations, one based on semi-empirical interatomic potentials (SEP) and the other on first-principles electronic structure (LDA). The former is done primarily to establish convergence criteria for the system size and ensemble sampling (see Section 2 of the Supplemental Material). Details of the LDA calculation (in-

cluding k-pt sampling [10]) are included in Section 1 of the Supplemental Material. While our moment calculations are purely classical, we use a simple physical argument to incorporate an estimate of quantum effects. The overall approach is novel in the following ways:

- is numerically efficient in that the calculations are relatively fast,
- is non-perturbative, in that it incorporates all higher order force constants implicitly, and
- applies a quantum correction to the classical calculations to account for phonon freezing at low temperatures.

As expected, the LDA calculations match more closely the experimental observations than do the SEP calculations. We confirm that the shifts are dominated by anharmonic effects beyond those that can be attributed to thermal expansion. The current results provide motivation to extend the method to include fourth moment, which can be done at minimal additional cost.

This paper is organized as follows. In Section II, we briefly review the theoretical approach, which is a second-moment calculation of the mode frequencies that is fully anharmonic. We introduce a quantum correction to the classical calculations to account for the phonon freezing at low temperatures. In Section III, we show the results when the calculation is based on interatomic potentials (Tersoff) and also results for first-principles LDA calculations using pseudopotentials. The calculations are done with and without thermal expansion, to evaluate the merits of the often-used quasi-harmonic approximation. In Section IV, we compare to experiments, and briefly point to further improvements that could be made at minimal additional cost. In Section 2 of the Supplement, we examine various convergence issues, and also demonstrate how the moments method easily and fully accounts for higher order anharmonicity. This work demonstrates that the moments method should prove to be an excellent exploratory tool for materials much more complex than silicon.

II. THEORETICAL METHOD

A. Basic approach and implementation

Our calculations of mode frequencies at various temperatures are accomplished via the second-moment approximation introduced by Dickel & Daw [11, 12] and further explored by Gao et al. [13, 14]. We give a brief review of this here, but refer the reader to the earlier papers for fuller treatment. The method is based on analysis using the Liouvillian, which is the operator that evolves functions in phase space according to a Hamiltonian

$$\hat{L} = i\{H, \}$$

(expressed using Poisson brackets). The Liouvillian is a linear operator even when the Hamiltonian contains a non-linear potential. For a system that is weakly anharmonic, the normal mode amplitudes should form a good basis for study. The autocorrelation of the amplitude A of normal mode γ in a given ensemble (for example, canonical) is given by

$$\chi_{\gamma}(t) = \frac{\langle A_{\gamma} e^{-i\hat{L}t} A_{\gamma} \rangle}{\langle A_{\gamma}^2 \rangle}$$

where the angular brackets indicate ensemble averages. The mode-resolved density of states (DOS) related to this autocorrelation

$$n_{\gamma}(\omega) = \frac{\langle A_{\gamma}\delta(\omega - \hat{L})A_{\gamma}\rangle}{\langle A_{\gamma}^2\rangle} \tag{1}$$

should correspond to the experimentally observed lineshape in neutron scattering. The term "moment" refers to the moments of the DOS as a function of frequency. Integrating $\omega^m n(\omega)$ from Eq. 1 gives

$$\mu_{m,\gamma} = \frac{\langle A_{\gamma} \hat{L}^m A_{\gamma} \rangle}{\langle A_{\gamma}^2 \rangle}$$

The idea is that the lineshape is generally very simple, so that low-order moments should give a reasonable representation of the shape. Furthermore, low-order moments are relatively easy to calculate, involving only displacements and forces. In particular, the mean frequency of normal mode γ should be approximately given by the second moment [14]

$$\omega_{\gamma}^2 = -\frac{\langle A_{\gamma} \ddot{A}_{\gamma} \rangle}{\langle A_{\gamma}^2 \rangle} \tag{2}$$

In practice, the ensemble averages are carried out via Metropolis Monte Carlo (MC). The \ddot{A} terms are obtained via the restoring force corresponding to that mode.

We note that this approximation is *not* the same as the often-discussed "quasiharmonic" approximation, where the harmonic frequency is calculated at an expanded lattice constant to take into account the effect of thermal expansion on the mode frequencies. Rather, even without thermal expansion, the second-moment calculation accounts for intrinsic anharmonicities through the ensemble averages. This point is discussed in more detail in Section 3 of the Supplemental Material.

We note the importance of the use of such mode ensemble calculations (as in Eq. 2) in the prediction of various material properties. In particular, Rudin [15] has recently used the correlation of such metrics to study soft phonon modes responsible for phase transitions from higher to lower symmetry crystal structures. While these averages were calculated in that work using full MD, the computational efficiency would likely be greatly improved through the use of MC calculations as we have used here.

We establish the normal mode basis for our approach by calculating the second-order force constant matrix for a given cell by making small displacements of each atom and cataloging the resulting Cartesian forces. The eigenvectors of the (zero-T) dynamical matrix form the projection operators that pull out the corresponding amplitudes and forces corresponding to each mode [14]. Because of the high symmetry of Si, the average of each normal mode amplitude is zero for all temperatures (so $\langle A_{\gamma} \rangle = 0$).

The MC calculations are carried out by stepping in the space of atomic displacements (sliding modes removed). To be more precise, the MC steps are performed in the normal mode space, because there we know the approximate width of the distribution at any temperature, given by the harmonic frequency. That is, for a weakly anharmonic system, $\langle A_{\gamma}^2 \rangle \approx \frac{k_B T}{m \omega_{\gamma}^2(0)}$ (where $\omega(0)$ is the harmonic frequency) should give us a good estimate of the most efficient step size to use for each mode. In the Metropolis algorithm, a candidate displacement is accepted or not depending on the change in energy it would incur. The step size was set this way so that the MC acceptance rate was uniformly about 70%. The restoring forces were computed for each accepted configuration. Note again that the anharmonicity of the system is incorporated automatically in the resulting set of displacements and corresponding forces. We do not decompose the energy into the usual second-, third-, and fourth-order force constants [16], but rather the full anharmonicity is incorporated in

a straightforward way. For the same reason, we do *not* decompose into the usual "normal" and "umklapp" processes [16], for those are also incorporated automatically, including the correct symmetry selection rules for the mode couplings. This results in a more robust formalism which implicitly includes the anharmonicity to every order in the proper way.

Required for this procedure are the energetics and forces corresponding to a particular set of atomic positions. In this work we obtain these in one of two alternate ways. The first set of calculations we report here is based on an interatomic potential for Si – the well-established Tersoff potential [17]. These were done with our previously reported JazzForLAMMPS code [18], which is a Python wrapper for LAMMPS [19]. The second set of calculations uses a driver developed for this purpose for the LDA code Quantum Espresso (QE) [20].

B. Quantum Correction

The Monte Carlo averages over the canonical ensemble that we do here are purely classical, which should be very reliable at high temperatures. However, at low temperatures the expected phonon freezing is easily observed in the experiments (glance, for example, at the experimental data in Figs. 2-4). As is well known, the transition between quantum and classical behavior is set by the Debye temperature. We propose here a method for accounting for quantum effects on anharmonic vibrational modes that allows us to extend our classical calculations to low temperatures as well. To our knowledge, this easy correction is a novel aspect to this work, but could be easily extended to other classical approaches beyond this moments approach.

Barron [21] noted that the frequency of vibrational modes would be altered by the presence of anharmonicity, and proposed that the shift should depend on the total vibrational energy in the crystal. In particular, he proposed that the lowest order anharmonicity should produce a shift in frequency of mode γ according to the harmonic vibrational energy per mode contained in all modes:

$$\omega_{\gamma}(T) = \omega_{\gamma}^{h} (1 - \frac{\langle E_{vib}^{h} \rangle}{3Nk_{B}\theta})$$

where ω^h is the harmonic frequency of the mode and θ is the temperature scale for anharmonicity assumed to be the same for all modes. Nelin and Nilsson [4], comparing to their experimental results on Si and Ge, proposed instead that each mode is differently sensitive

to the anharmonicity, so that θ is different for each mode:

$$\omega_{\gamma}(T) = \omega_{\gamma}^{h} (1 - \frac{\left\langle E_{vib}^{h} \right\rangle}{3Nk_{B}\theta_{\gamma}})$$

The behavior at all temperatures can be captured by the total energy of a set of quantum oscillators

$$\left\langle E_{vib}^{h} \right\rangle = \left\langle \sum_{\gamma} \hbar \omega_{\gamma}^{h} (n_{\gamma} + \frac{1}{2}) \right\rangle$$

where n_{γ} is the Bose-Einstein distribution function. Nelin and Nilsson followed a common simplification of approximating the sum by a single term, defining a mean frequency ω_g and incorporating the Bose-Einstein distribution function for that mean frequency:

$$\langle E_{vib}^h \rangle \approx 3N\hbar\omega_g \left(\frac{1}{e^{\hbar\omega_g/k_BT} - 1} + \frac{1}{2}\right)$$
 (3)

This approach accounts for the behavior over the full range of experimental temperatures. At high temperature the frequency of each mode is approximately linear in T with slope related to its θ . At low temperatures the anharmonicity affects the observed frequency:

$$\omega_{\gamma}(0) = \omega_{\gamma}^{h} \left(1 - \frac{\hbar \omega_{g}}{2k_{B}\theta_{\gamma}}\right)$$

This argument concludes that the low-temperature experimental frequency should not be compared directly to the harmonic frequency calculated, for example as we do here, from the eigenvalues of the dynamical matrix, but should incorporate a correction due to the anharmonicity present even in the zero-point motion.

The expression Nelin and Nilsson then compared favorably to their experimental results was

$$\frac{\Delta\omega_{\gamma}}{\omega_{\gamma}(0)} = \frac{-\hbar\omega_{g}}{k_{B}\theta_{\gamma}} \left(\frac{1}{e^{\hbar\omega_{g}/k_{B}T} - 1} + \frac{1}{2} \right) \tag{4}$$

where $\Delta\omega_{\gamma} = \omega_{\gamma}(T) - \omega_{\gamma}(0)$. At high temperatures this fractional frequency shift goes like $-T/\theta_{\gamma}$ and at low temperatures it flattens out. A further consequence of this analysis is that extrapolating the high-temperature frequency back to T=0 results in an intercept at a non-zero frequency. Or turned around another way, a purely classical calculation should be shifted in frequency by quantum effects in order to be compared to experiment.

To do this in our case, we would determine the slope of our results at high temperature, thereby fixing the predicted θ_{γ} for each mode, and then plot Eq. 4 to compare to experiment. But that is not quite sufficient for our calculations because – as we will see – we find some

small amount of higher-order anharmonicity that results in a small curvature at higher T rather than purely linear behavior. To account for this we extend the previous argument.

We return to the analysis where the frequency is proposed to be shifted linearly with the vibrational energy. Now we extend this to include terms quadratic in the vibrational energy as well, with a different sensitivity factor.

$$\omega_{\gamma}(T) = \omega_{\gamma}^{h} \left(1 - \frac{\langle E_{vib}^{h} \rangle}{3Nk_{B}\theta_{1,\gamma}} - \left(\frac{\langle E_{vib}^{h} \rangle}{3Nk_{B}\theta_{2,\gamma}}\right)^{2}\right)$$
 (5)

This adds an even smaller correction due to higher anharmonicity. The frequency at T=0 is

$$\omega_{\gamma}(0) = \omega_{\gamma}^{h} \left(1 - \frac{\hbar \omega_{g}}{2k_{B}\theta_{1,\gamma}} - \left(\frac{\hbar \omega_{g}}{2k_{B}\theta_{2,\gamma}}\right)^{2}\right)$$
 (6)

At high temperatures there should be a largely quadratic dependence on T.

Our procedure is then to determine the two constants $\theta_{1,\gamma}$ and $\theta_{2,\gamma}$, representing the firstand second-order anharmonicities, for each mode from our purely classical calculations. From the classical limit of Eq. 5, we get

$$\frac{\omega_{\gamma}(T)}{\omega_{\gamma}^{h}} - 1 = -\frac{T}{\theta_{1,\gamma}} - (\frac{T}{\theta_{2,\gamma}})^{2}$$

which we use to fit our classical calculations. Then we use Eqs. 3, 5 and 6 to correct our classical calculations for quantum effects. In this, we used the Debye frequency for ω_g , though we note that the resulting curves are not sensitive to this choice. In this way, our classical calculations can be compared more directly to the experiments. The main effect of these corrections is to impose the freeze at lower temperatures and to offset at higher temperatures the plot of the fractional frequency shift upwards.

This quantum correction to the presently purely classical calculations is quite general, and could be also used in calculations not based on the moments approach.

III. RESULTS

We show now the results we have obtained using calculations based on the two sources for energies and forces: (1) semi-empirical potential (SEP, Tersoff's form), and (2) LDA. Details of the LDA calculations are given in Section 1 of the Supplemental Material, and convergence with respect to MC sampling, cell-size, and (for LDA) k-points and cut-off energy are discussed in Section 2 of the same.

TABLE I: Harmonic frequencies for particular modes calculated using semi-empirical potential (SEP) and with LDA in the 8-atom cell described in the text. Frequencies are in THz. Experiment values are from Dolling [22]

mode	SEP	LDA	Xpt
TA(X)	7.0	4.1	4.5
L(X)	12.1	12.3	12.0
TO(X)	15.0	13.8	13.7
$\mathrm{O}(\Gamma)$	16.0	15.5	15.4

TABLE II: The two anharmonicity parameters for each mode used to estimate quantum effects. (See Section II.B)

mode	$\theta_1(K)$	$\theta_2(K)$
TA(X)	23347	5581
L(X)	22900	5920
$\mathrm{O}(\Gamma)$	15834	5525

We focus on high-symmetry modes commonly reported by experiment. At k=0 (Γ -pt.) there are three sliding modes at zero frequency and three optical modes that we designate as $O(\Gamma)$. At $k=(\pi/a,0,0)$ (X-pt.) there are three distinct sets of modes: a transverse acoustic mode (which we refer to as TA(X)), a degenerate mode which is both longitudinal acoustic and longitudinal optical (which we call L(X)), and transverse optical mode (denoted TO(X)). Our computed harmonic frequencies (corresponding to the zero temperature, classical limit) for these modes for both SEP and LDA are shown in Table I and compared to well-referenced experimental data.[24] We note, though, that it is not the harmonic frequencies that we are after but the more challenging anharmonic shifts in those frequencies.

To estimate the quantum effects (Section IIb) we fit to the high temperature slope and curvature of our classical calculations. In Table II we show the anharmonicity parameters so determined. These numbers are used, along with the Debye frequency, to determine the quantum corrections.

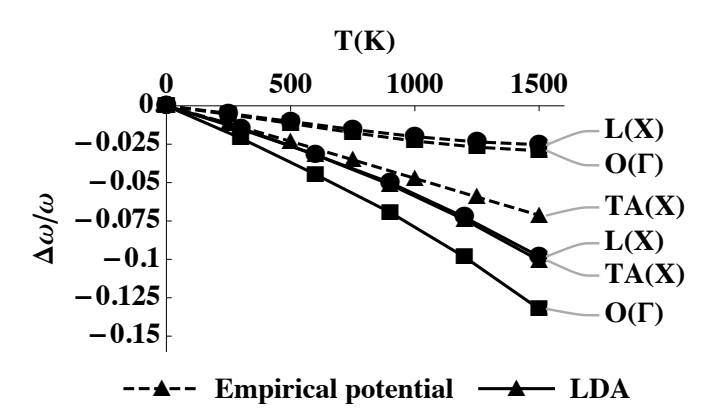


FIG. 1: The normalized frequency change $(\Delta\omega/\omega)$ for each of the modes discussed in the text as functions of temperature. This figure shows results that incorporate thermal expansion using experimentally determined expansion. The results in this figure are purely classical (that is, do NOT incorporate the quantum correction from Section II.B) The solid lines indicate calculations done using LDA, and the dashed lines show calculations done using the SEP. The two sources show similar downward trends but opposite curvatures.

In Fig. 1, we show the temperature dependence of the frequencies by plotting $\frac{\omega(T)-\omega(0)}{\omega(0)}$ for each of the modes discussed here. These results incorporate thermal expansion using experimentally determined expansion, but in this figure are purely classical (that is, do not incorporate the quantum correction from Section II.B). The LDA calculations (solid lines) trend downward, with all modes at roughly the same decrease and some gentle negative curvature, with the $O(\Gamma)$ mode being most sensitive to temperature. The SEP calculations (dashed lines) show the TA(X) mode as standing out from the others, with the other three showing some small amount of upward curvature. Naively the downward trend shows a softening of all modes with increasing temperature, which is due (as we discuss more later) not to thermal expansion but in other ways due to the anharmonicity of Si. The difference in curvature between SEP and LDA is noted and discussed more fully in Section 3 of the Supplemental Material.

We see that the fractional shifts are of approximately the same size for all modes. This is consistent with the overall squeezing down of the DOS that is seen with increasing temperature, maintaining its overall shape. It is pointed out by Kim *et al.* [5, 6] that this resembles what one might expect from an overall softening of the lattice due to thermal expansion. However, their detailed analysis leads them to conclude otherwise: that the shifts seen with

increasing temperature are much larger than what can be attributed quantitatively to simple thermal expansion (or the quasi-harmonic approximation).

As an independent – and more direct – test of the argument presented by Kim et al. regarding the quasi-harmonic approximation, we did calculations both at constant volume (at the optimized LDA lattice constant) and incorporating thermal expansion (using the experimental values for thermal expansion coefficient). At T=1200K, the lattice constant of Si is observed to be increased from its low temperature value by a factor of 1.003. We find that our results are not sensitive to thermal expansion. Using the low-temperature lattice constant for our MC calculations at T=1200K would change our fractional shifts for the TA(X) mode by 27%, for L(X) by 8%, and for $O(\Gamma)$ by 5%. Thus the effects of thermal expansion on the values of the fractional shifts are minor. The large majority of the frequency shift is due then to intrinsic anharmonicity of the Si lattice, not due to the thermal expansion.

IV. COMPARISON TO EXPERIMENTS

In Figs. 2-4 we show the LDA results with and without the quantum correction from Section II.B, and also compare to experiment [25]. These results include thermal expansion based on the experimental values for the expansion coefficient. The agreement between theory and experiment is excellent for the TA(X) mode, and is very similar to that obtained by a more expensive means in Kim et al. [6]. However, for the $O(\Gamma)$ mode the results are less good, though agree with the experimental shifts to within a factor of two. Given the simplicity of the second-moment approximation (Eq. 4) and the relative ease of implementation and low cost of calculations, we suggest that the overall agreement is acceptable. (The reader is asked to note that Kim et al. reported only results for the low frequency transverse acoustic modes in order to build the case against the quasi-harmonic approximation that is a principal theme of their work. However, they do not show a comparison the higher-frequency longitudinal acoustic and optical modes as we do here. Their agreement for the low-frequency transverse acoustic modes is comparable to the agreement we report here.)

From these results, we see that the second-moment approximation is good enough to get to within a factor of 2 of the frequency shift, as we saw with our previous work on carbon nanostructures [7, 8]. For better agreement it seems necessary to include the next moment

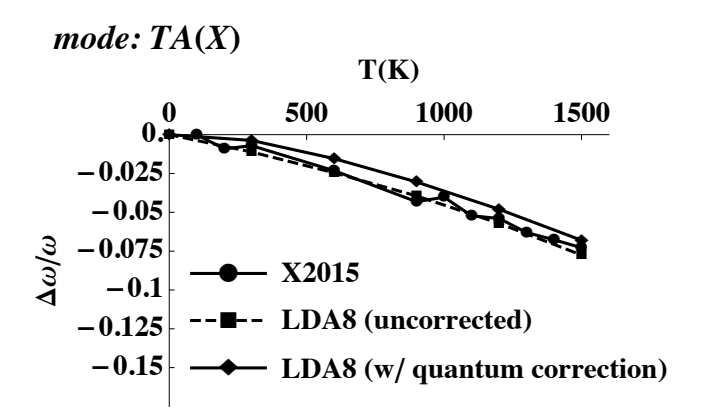


FIG. 2: Fractional frequency shift with temperature of the TA(X) mode, with and without quantum correction, compared to experiment [5]. The calculations are done with experimental values for the thermal expansion.

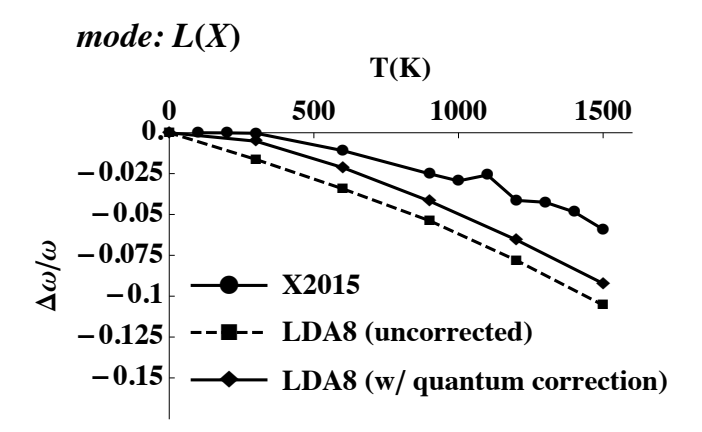


FIG. 3: Fractional frequency shift with temperature of the L(X) mode, with and without quantum correction, compared to experiment [5]. The calculations are done with experimental values for the thermal expansion.

(fourth). The fourth moment can be written $\langle \ddot{A}_{\gamma}^2 \rangle$. This can be obtained also from the forces that we have calculated already and so will not increase the computational time. This is good ground for future work.

V. CONCLUSIONS

We have presented moments calculations of the temperature-dependence of the normal mode frequencies over a range of temperatures up to 1500K. The calculations are based on ensemble averages of displacements and forces calculated using two different representations

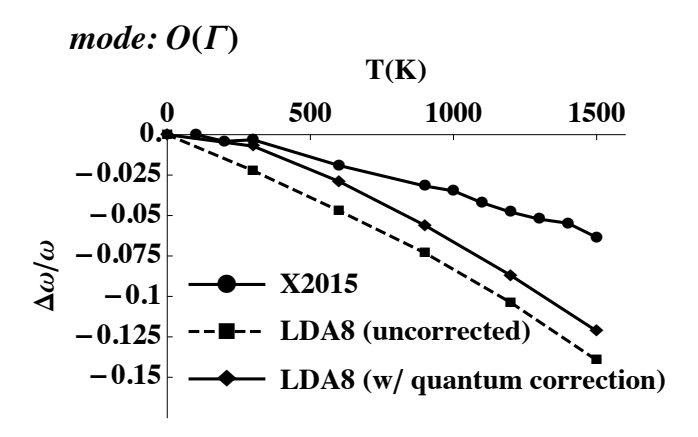


FIG. 4: Fractional frequency shift with temperature of the $O(\Gamma)$ mode, with and without quantum correction, compared to experiment [5]. The calculations are done with experimental values for the thermal expansion.

of the intrinsic interactions of Si – semi-empirical, Tersoff-style potentials and first-principles electronic structure (LDA) calculations. The former are used to establish convergence with respect to cell-size and MC sampling. The latter are expected to be more reliable quantitatively. Our calculations incorporate all interactions nonperturbatively, without the need for explicitly calculating higher-order force constants. This is in contrast to, for example, the theoretical treatment considered by Kim et al. [6] and Shulumba, Hellman, and Minnich [23], where a force field model is considered at each temperature with parameters adjusted to match first-principles calculations to determine the normal mode frequencies. Our moments method determines a frequency at temperature directly from the first principles calculations, without resort to a model. These MC calculations are much more efficient compared to MDbased approaches. We also incorporate an estimate of expected quantum effects to enable direct comparison of our otherwise classical calculations to experiment. The first-principles shifts agree to within a factor of 2 with recent inelastic neutron scattering data. We suggest that even better agreement with experiment could be obtained by incorporating fourth moment, which is proposed for future work. Noting the relative simplicity and speed of the calculations, we conclude that the second-moment approximation reasonably accounts for anharmonicity beyond what can be predicted using quasi-harmonic methods in a system that has been very closely studied and may reasonably be used to explore more complex systems.

VI. ACKNOWLEDGEMENTS

Clemson University is acknowledged for generous allotment of compute time on its Palmetto cluster for this and other projects. We thank Mr. Andrew Garmon (Clemson) and Mr. Ashwin Trikuta Srinath (Clemson) for helpful suggestions during this work relating to the Palmetto cluster. We also thank Dr. Dennis Kim (currently at UCLA) and Dr. Brent Fultz (CalTech) for discussions relating to their work. One of us (MSD) was supported by the U. S. Department of Energy, Office of Basic Energy Science, Division of Materials Sciences and Engineering under Grant DE-SC0008487.

[1] T. R. Hart, R. L. Aggarwal, and B. Lax, Phys Rev B 1 638 (1970).

- [7] H. Wang, D. Dickel and M. Daw, J. Raman Spec. 49 621 (2018).
- [8] H. Wang and M. Daw, Computational Mat. Sci. **146** 70 (2018).
- [9] H. Wang and M. Daw, Phys Rev B **94** 155434 (2016).
- [10] H. J. Monkhorst and J. D. Pack, Phys. Rev. B 13 5188 (1976).
- [11] D. Dickel and M. S. Daw, Computational Mat. Sci. 47 698 (2010).
- [12] D. Dickel and M. S. Daw, Computational Mat. Sci. 49 445 (2010).
- [13] Y. Gao, D. Dickel, D. Harrison and M. Daw, Computational Mat. Sci. 89 12 (2014).
- [14] Y. Gao and M. Daw, Modeling and Simul. Mater. Sci. Eng. 22 075011 (2014).
- [15] S. Rudin, Phys Rev B **97** 134114 (2018).
- [16] O. Madelung, Introduction to Solid State Theory (Springer-Verlag, New York, 1978).
- [17] J. Tersoff, Phys. Rev. B, **39** 5566 (1989); Erratum: Phys. Rev. B **41** 3248 (1990).
- [18] Y. Gao, H. Wang, and M. Daw, Modeling and Simul. Mater. Sci. Eng. 23 045002 (2015).

^[2] M. Balkanski, R. F. Wallis, and E. Haro, Phys Rev B 28 1928 (1983).

^[3] J. Menendez and M. Cardona, Phys Rev B 49 2051 (1984).

^[4] G. Nelin and G. Nilsson, Phys Rev B **10** 612 (1974).

^[5] D. S. Kim, H. L. Smith, J. L. Niedziela, C. W. Li, D. L. Abernathy, and B. Fultz, Phys Rev B 91 014307 (2015).

^[6] D. S. Kim, O. Hellman, J. Herriman, H. L. Smith, J. Y. Y. Lin, N. Shulumba, J. L. Niedziela, C. W. Li, D. L. Abernathy, and B. Fultz, Proc Nat Acad Sci 115 1992 (2018).

- [19] S. Plimpton, J Comp Phys 117 1 (1995). We used the version dated 1 Feb 2014.
- [20] P. Giannozzi et al. J.Phys.:Condens.Matter 21 395502 (2009). P. Gianozzi et al.
 J.Phys.:Condens.Matter 29 465901 (2017). We used PWSCF version 5.4.0.
- [21] T. H. K. Barron, Lattice Dynamics: Proceedings of an International Conference in Copenhagen (Pergamon, New York, 1965) p. 247.
- [22] G.Dolling, Inelastic Neutron Scattering Vol.2, p37 (IAEA Vienna 1963).
- [23] N. Shulumba, O. Hellman, and A. J. Minnich Phys Rev B **95** 014302 (2017).
- [24] Because the vibrational dispersion curves of Si have been studied so extensively, and because Si is such a textbook material and the dispersion relations given in many introductory books on solid state physics, we will not show here the detailed dispersion curves using the SEP and LDA. We refer the interested reader instead to textbooks (e.g., see M. Marder Condensed Matter Physics (Wiley, 2000) and C. Kittel Introduction to Solid State Physics (Wiley, 1996)) and what has become classic experimental (e.g., see G. Dolling and R. A. Cowling Proceedings of the Physical Society (London), 88 pp 463-504 (1966), G. Nilsson and G. Nelin, Phys Rev B 6 3777 (1972), and W. Weber, Phys Rev B 15 4789 (1977).) and theoretical literature (e.g., S. Wei and M. Y. Chou, Phys Rev B 50 2221 (1994) and A. Rohskopf, H. Seyf, K. Gordiz, T. Tadano and A. Henry, Computational Materials 3 27 (2017).)
- [25] The available experimental data (Raman [1–3] and neutron scattering [4–6]) are very consistent with each other. We compare here to the neutron scattering results on powders [5] because the published data are more complete in that paper, but the comparison to the other data would be very similar.